FASTR: Flexible Articulating Surgical Transoral Robot

Major Qualifying Project

Submitted By:

Chase Beausoleil, Biomedical Engineering and Robotics Engineering
Mark Gagliardi, Electrical and Computer Engineering and Robotics Engineering
Samay Govani, Mechanical Engineering and Robotics Engineering
Cole Parks, Computer Science and Robotics Engineering

Project Advisors:

Prof. Loris Fichera
Prof. Stephen Bitar
Prof. Yuxiang Liu

Worcester Polytechnic Institute

Aug 2023 - May 2024

Abstract

Transoral Robotic Surgery (TORS) is a promising minimally invasive approach for the treatment and removal of microlaryngeal tumors, offering enhanced precision and reduced clinician fatigue over manual methods. The Da Vinci Single Port Surgical System is the only commercially available and FDA-approved robotic system for TORS. However, the high cost and remote center of motion limit the widespread adoption of the Da Vinci system.

To provide an enhanced method for laryngeal surgery, a new system is required to perform TORS in the glottis region of the larynx where the workspace is constrained and the surgical tools need to be inserted orally.

In this paper, we present FASTR, a novel robotic system for TORS that is more cost-effective and less invasive than the Da Vinci system. The proposed system consists of two sub-systems: a 3-DOF robot consisting of two cylindrical tubes connected by a cable-driven flexible joint, and concentric tube continuum robots that sit inside the tubes of the 3-DOF robot. The 3-DOF robot is used to position the concentric tube continuum robots in the desired surgical workspace while the concentric tube continuum robots hold the surgical tools and provide the necessary dexterity for the surgical procedure.

ACKNOWLEDGEMENTS

This Major Qualifying Project was supported by the Cognitive Medical Technology Laboratory (COMET Lab) at Worcester Polytechnic Institute (WPI). We appreciate the support they have provided throughout the course of this project.

Additionally, we would like to thank our advisors, Professor Stephen Bitar, Professor Yuxiang Liu, and especially Professor Loris Fichera, for their guidance and mentorship throughout our design process.

We would like to thank Dr. John E. Hanks, MD for his clinical expertise and for providing us with the foundation for this project.

TABLE OF CONTENTS

List of Tables

Table **Page**

List of Figures

CHAPTER 1

INTRODUCTION

In the year 2023, there were approximately 12,380 newly reported cases of laryngeal cancer, with an estimated 90,000 individuals living with this condition [6]. Presently, surgeons commonly employ narrow and elongated tools to extract tumors from patients' laryngeal cavities. However, the use of such tools often forces surgeons into awkward ergonomic positions, leading to frequent hunching over or leaning back during surgical procedures. Beyond the ergonomic challenges, the throat's inherently confined space limits visibility for surgeons, even when utilizing a laryngoscope to widen the patient's throat. This constrained environment provides minimal room for maneuvering surgical instruments, further complicating the intricacies of laryngeal cancer surgeries.

1.1 Current Surgical Procedure

Various forms of laryngeal surgery exist, but micro laryngeal surgery stands out, utilizing small tools and navigating through confined spaces. This specialized approach is preferred for its minimal impact, often allowing for outpatient procedures that don't require extended hospital stays [7]. The first step in any micro laryngeal surgery is the application of general anesthesia [8]. After the patient is under anesthesia and in a supine position, the patient's head is titled backwards and a metal laryngoscope is inserted through the oral cavity as shown in Figure 1.1. A laryngoscope is a medical instrument used to directly view the larynx. It comprises two parts: a shorter, curved section that is securely held outside the patient, and a longer section that is inserted into the patient's throat. The soft tip of this longer section reaches the larynx. Figure 1.2 shows a typical laryngoscope, while Figure 1.3 displays the dimensions of a standard adult laryngoscope. The size of the laryngoscope varies depending on the patient's throat size and age.

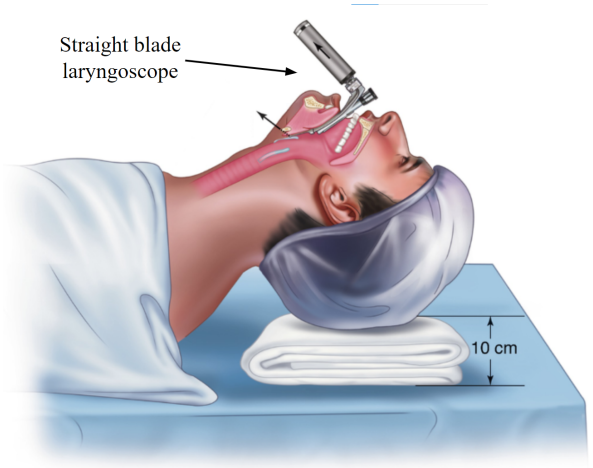

Figure 1.1: *Insertion of straight blade laryngoscope into patient's throat. Reproduced from [1].*

Figure 1.2: *A typical micro-laryngoscope with a soft point at its distal end*
Netha Hussain, CC BY-SA 4.0, via Wikimedia Commons.

Once the laryngoscope is inserted, it is fixed in place via a mounting bracket placed on a medical cart that remains in place for the duration of the surgery. This concludes the procedural setup for most laryngeal surgeries. Following laryngoscope insertion, long, narrow tools (often spanning 25-30 centimeters in length [2]) as shown in Figure 1.4 are inserted through the laryngoscope and a magnifying lens is used by the operating physician to view the instruments in the surgical context and perform surgery, shown in Figure 1.5.

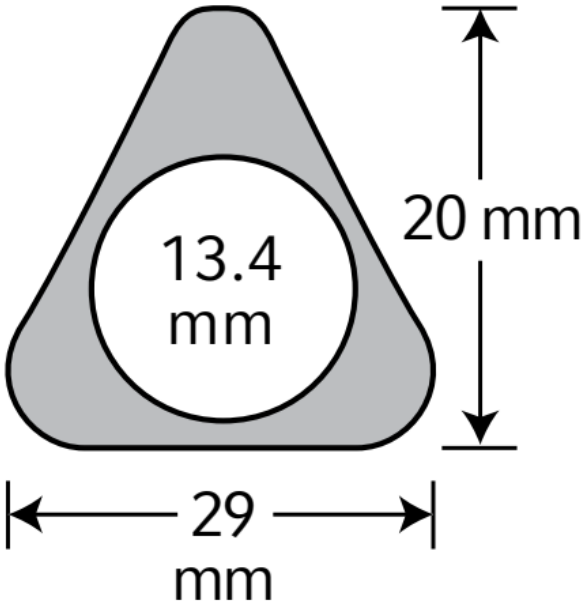

Figure 1.3: *Typical adult laryngoscope cross-section. Reproduced from [2].*

Figure 1.4: *Micro laryngeal grasping forceps.*

As depicted in Figure 1.5, the surgeon is observed hunching over to achieve a clearer view through the rigid endoscope. The use of long, narrow tools in conjunction with a confined surgical workspace and limited visibility can contribute to surgeon fatigue. An evaluation of micro laryngeal operating procedures highlights that otolaryngologists are particularly susceptible to musculoskeletal disorders, as indicated by [9]. This underscores the importance of ergonomics and proper positioning in surgical settings to minimize the risk of long-term physical strain and injuries. Implementing ergonomic practices and using specialized equipment designed to reduce strain can significantly improve both the comfort and effectiveness of microlaryngeal procedures for surgeons.

Figure 1.5: *Otolaryngologist maneuvering direct endoscope through laryngoscope. Reproduced from [3].*

1.2 Existing Robotic Surgery Devices for Laryngeal Procedures

Very few robotic surgery systems have been utilized for laryngeal procedures for a variety of reasons including: cost, insufficient dexterity, and relatively large instrument size. Lying at the core of the lack of adaptation of robotics for micro laryngeal surgery is the large instrument size, the Da Vinci robots were designed for thoracic and abdominal surgeries where the workspace is much larger and the robot's arms better mimic the behavior of a surgeon's motions [10]. In a case study looking at the use of the Da Vinci robot for a laryngeal surgery, it was noted that the laryngoscope the surgeons used, *"only provided operative space for one 8-mm robotic arm in addition to the 12-mm stereoscopic camera"* [10]. Naturally, inserting a rigid link robot such as the Da Vinci robot introduces a remote point of rotation at the end of the surgical device, severely limiting dexterity [11]. The crowding of instrumentation within the surgical workspace also decreases or eliminates the ability of the operating physician to remove the robotic system and operate manually in the case of an emergency. Lastly, the cost of the Da Vinci system is prohibitive to many hospitals as solely a laryngeal procedure tool and would have to be used for multiple applications, leading to less uptime and use in laryngeal procedures.

While there are multiple disadvantages posed by traditional robotic surgery systems such as the Da Vinci, a few key components of the Da Vinci system prove to be useful for micro laryngeal applications specifically. Firstly, 3D imaging of the surgical workspace comes with numerous benefits such as decreased strain on the operating physician's back due to not using a microscope anymore, and more information is available to the surgeon as well as the medical staff which ultimately provides better and more immersive surgical experience [12].

1.2.1 Soft Robotics for Surgical Devices

Soft Robotics are a broad class of robots with flexible spines that are typically deformed via some form of remote actuation (cables, microfluidics, pneumatics, etc.) to result in some end effector position. These devices offer numerous benefits over traditional rigid robots for the purpose of minimally invasive surgeries. For one, soft robots lower the risk of inadvertent damage since the only component capable of cutting, cauterizing, or impacting body tissue is at the tip of the soft robotic end effector. Further, soft robots can be designed to curve continuously, which allows for more complex motion in tight spaces such as the larynx [11]. Lastly, soft robots often can be manufactured using consumer-grade materials, which are inexpensive when compared to their rigid counterparts.

There are however some disadvantages in using soft robots in surgical applications. The most important of which is low force exertion. The force required to deform a soft robot is inversely related to the force the soft robot can apply to a medium prior to deforming inadvertently [11]. Meaning, a soft robot which could hold a position with a large holding force often requires a large actuation force. However, microlaryngeal procedures often deal with soft, delicate tissue with

little required force to manipulate the tissue desirably. Next, task-space control and kinematics of soft robotics is often computationally expensive and nonlinear in nature. While it is true that task space control is significantly more intuitive for operating physicians [13], soft robots that deform with constant curvature are relatively easier to understand from a surgeon's perspective.

1.3 Paper Outline

This paper begins by providing an overview of microlaryngeal surgery, covering the instruments used and any special considerations

Next, the paper introduces a novel multi-stage laryngeal surgery robot. This innovative system comprises a soft robotic outer sheath delivering two cameras, combining to form a stereo camera, along with three soft robotic manipulators equipped with tool heads for simultaneous use in the surgical workspace.

The subsequent section presents the project's results and incorporates feedback from a trained ENT surgeon, offering valuable insights. The paper concludes by looking ahead, discussing future work and potential advancements in robotic-assisted laryngeal surgery. This concise journey encapsulates the development, evaluation, and future prospects of the presented surgical technology.

CHAPTER 2

PRELIMINARY STUDY: EXISTING SURGICAL TECHNIQUES

2.1 Client Statement

The goal of this project was to create a novel solution for transoral robotic microsurgery in the context of laryngeal procedures. Dr. John Hanks, MD, a collaborator on this project, provided insight into the medical aspects and implications of robotic surgery, as well as current manual procedures. The lack of maneuverability in the confines of the larynx's small workspace has been expressed by Dr. Hanks as a major concern and has been a large focus of innovation for this project.

2.2 Relevant Anatomy

The larynx is a hollow tube that is part of the respiratory system and is made up of cartilage, muscles, and ligaments [14]. This tube is approximately four to five centimeters in length and width and is located in the neck below the oropharynx, in front of the hypopharynx, and above the trachea between the C3 and C7 vertebrae [15]. Multiple cartilaginous structures make up the larynx, including the thyroid cartilage [16]. The larynx can be broken down into three sections, including the supraglottis, the glottis, and the subglottis [14]. The supraglottis is located at the top of the larynx and most notably contains the epiglottis, which is a small flap of elastic cartilage that moves to cover the top of the larynx when an individual swallows. The epiglottis works to stop consumed food and fluid from accessing the larynx and continuing into the trachea and the lungs. When an individual is not swallowing, the epiglottis remains open and the air is able to move into the larynx, through the trachea, and further into the lungs [17].

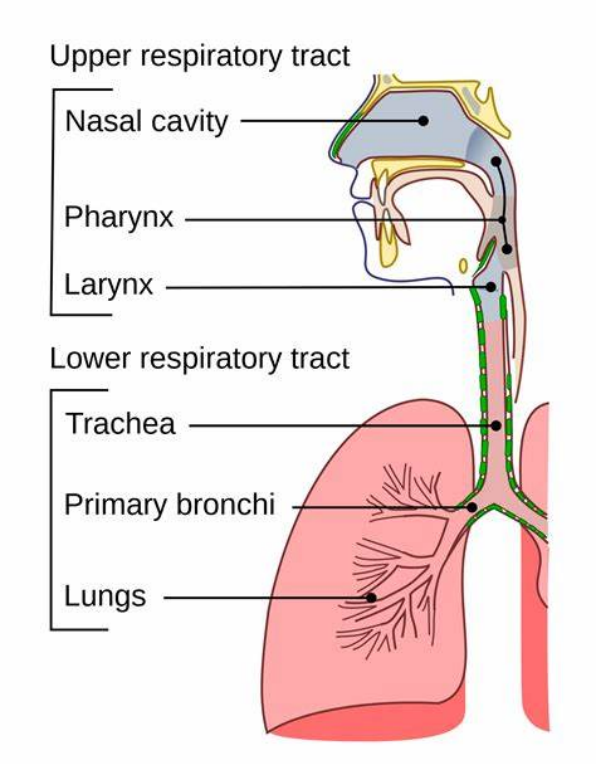

Figure 2.1: *The upper respiratory tract, containing the larynx, where the vocal cords are anatomically located. Reproduced from [4].*

Located directly below the supraglottis is the glottis, which is the section of the laryngeal cavity that comprises the vocal cords and the cause for the larynx colloquially being termed the voice box [14]. The vocal cords consist of four folds of fibro-elastic tissue, which are further differentiated into the superior vocal cords and the inferior vocal cords. The two superior vocal cords are thin, contain no muscle, and are also known as the false vocal cords. The inferior vocal cords are wide, muscular, and termed the true vocal cords due to their ability to join and separate [15].

The subglottis makes up the inferior section of the larynx and connects to the superior region of the trachea [15]. Similar to the supraglottis, the subglottis is cylindrical but smaller near the glottis region of the larynx. The diameter of the subglottis expands as it extends caudally to the trachea [18].

Most cancers that occur in the larynx and throat are squamous cell carcinomas, as the lining of the throat is composed of squamous cells [19]. Usually, laryngeal cancer originates in the glottis but can expand into the other regions of the larynx and to other parts of the body. Symptoms of laryngeal cancer may include a lump in the neck, difficulty swallowing, hoarseness in the voice, or a change in the voice [15].

2.3 Existing Methods for Laryngeal Procedures

Endoscopy has become the preferred method for a variety of examinations and surgical procedures. Endoscopic approaches are meant to be minimally invasive as compared to the open surgery equivalents. The anatomy of the neck is complex and dense, consisting of many important nerves and vascular and lymphatic structures. During open surgery of the neck, these vital structures must be identified and preserved to avoid potentially fatal complications. Other non-fatal complications may cause long-lasting consequences for the patient. Despite expert knowledge of the relevant anatomy, the complexity and density of this region presents many opportunities for surgical complications during open surgery. Oral laryngoscopy is a specific type of endoscopy that involves inserting an endoscope and tools through the mouth and directing them down the throat to the area of the larynx. The purpose of this procedure is to transverse past the epiglottis to the location of the vocal box, and thus examine or perform an operation on and around the vocal cords. Currently, there are multiple endoscopic options for laryngeal procedures. Understanding the existing techniques and their associated advantages and disadvantages allows for the potential improvement in laryngoscopy.

Transoral Laser Microsurgery (TLM) is a procedure that utilizes a laser to make incisions in a patient's mouth or throat. Significant research has been performed to understand the viability of the technique in the context of laryngeal surgeries. A study completed on using TLM for laryngeal cancer determined that TLM has a lower complication probability than open surgery [20]. Postoperative hemorrhaging is still a concern with TLM, but it is much less likely in comparison to a more invasive open surgery.

Transoral Robotic Surgery (TORS) refers to the utilization of any robotic system to execute a procedure via the oral cavity. The most well-known and only FDA-approved robotic system for this type of surgery is the Da Vinci Single Port (SP) surgical system [21]. The single port consists of 3 robotic arm tools and a video endoscope [22].

Figure 2.2: *The Da Vinci System. The Single Port version consists of only one arm (of the four in the image) carrying three robotic tools and a video camera. Reproduced from [5].*

Case studies have been performed on human or animal cadavers to study the efficacy of robotics to laryngeal procedures. Hockstein et al. describes their findings with regard to using the da Vinci for TORS on a human cadaver [23]. While performing laryngeal and pharyngeal surgeries, they found more precise results than manual endoscopic surgery. This was credited to the improved vision, control, and tool movement that the da Vinci system provided. It was especially noted that the degrees of freedom of the da Vinci system's instruments significantly increased the surgeon's workspace. The use of TORS was found to aid in preventing instances where manual endoscopic methods would be deemed insufficient and a surgeon would need to resort to invasive open neck surgery intraoperatively.

The Da Vinci system has made strides in performing TORS in the different regions of the pharynx and, additionally, the epiglottis and supraglottis [21]. However, some aspects of TLM are currently superior to transoral surgery performed using the Da Vinci. A study published in 2013 compared the first ten patients of TLM and the first ten patients of TORS for supraglottic cancer [24]. One conclusion from the study was that postoperative dysphagia, or difficulty swallowing after surgery, was worse on average for TORS patients than TLM patients. Postoperative dysphagia is a complication following esophageal or laryngeal surgery that may cause difficulty swallowing, respiratory deterioration, and even death. Although breakthroughs were seen in TORS, the study believed that TORS needs more time to develop to completely surpass TLM as the default method for laryngeal surgeries; this was merely because TLM is an earlier approach of transoral surgery. In another study where laryngeal procedures were performed on canine cadavers, TORS was found to be superior to TLM in terms of visibility and maneuverability. This was especially noticeable in the event of visual repositioning as the individual camera arm of da Vinci could be adjusted instead of the entire apparatus with the camera fixed to the laryngoscope in TLM [23] [25]. TORS was also found superior to TLM in resecting larger-sized tumors [25].

Despite various advantages of TORS and TLM, both surgical methods exhibit limitations, most notably in visibility and maneuverability. Schild et al. states that the available tools for TORS are too restrictive in movement, while TLM is currently held back by the line of sight requirements of the laser [26]. In another case study published by Hockstein et al. where they alternatively used an airway mannequin, challenges were expressed with TORS. Mainly, the inability to use a laryngoscope makes it difficult for the insertion of the robotic arms [27]. One common recommendation made was to improve TORS by reducing the size of the robotic tools to improve optical and reachable exposure [28] [25]. Yet another drawback of TORS is the current absence of haptic feedback. Without this type of surgeon-patient interaction, surgeons lack the ability to understand the pressure at which they palpate, thus resulting in more uncertainty about a tumor. Further shortcomings of TORS include its reliability in select cases. Poor exposure has been the cause in TORS surgeries for resorting to an open surgery approach or even procedure abandonment [29]. Solares and Strome further supported the unreliability of robotic surgery when using a robot-assisted transoral laser method. Two out of three attempted surgeries could

not be completed, and manual strategies had to be applied [30]. Regardless of studies concluding better exposure in TORS as compared to manual endoscopic approaches or TLM, the presence of cases abandoning robotic surgery emphasizes a continued inadequacy of exposure.

2.4 Existing Instruments for Laryngeal Procedures

A laryngoscope is the most widely used tool to provide access to a patient's larynx during surgery. Most laryngoscopes are rigid, made of stainless steel, and designed to be fixed in a patient's throat for the duration of the surgery. They are hollow to allow tools to pass through to the larynx for control outside the body. Different surgical applications and anatomical considerations require different shapes and sizes of laryngoscopes and although the largest laryngoscope to fit is typically preferred, surgeons have found that smaller sizes are more practical to improve exposure of the larynx and prevent injuries on insertions [25]. It should also be noted that the majority of laryngoscopes support the attachment of illumination and fluid evacuation tools on the outside in addition to the tools traversing a laryngoscope internally [25].

Most surgical tools used in manual laryngeal surgeries consist of a millimeter-scale tool head, a shaft close to twice the length of laryngoscopes, and a handle that resembles that of scissors to allow for manual actuation of the tool head, as seen in Figure 1.4. A wire from the scissors handle traverses the shaft to the tool head, allowing for the actuation of the tool head when the scissors handle is manipulated. A variety of tools exist for specific surgical applications that are presented during laryngeal procedures. These tools include sickle knife and scissors, which are used to resect tissue and utilize different blade types for different cutting angles and tumor shapes. Based on inputs from our clinical collaborator, forceps are another common tool and are used to grab and retract tissue in the context of improving visualization or providing pressure when resection is occurring. Furthermore, some tools exhibit a tool head and shaft but not the scissors handle as they do not require actuation. Such tools include blunt tools, which are used to palpate or manipulate tissue, especially cancers that are not mobile. Blunt tool heads do not require actuation and therefore do not require scissor handles at the opposite end of the shaft they are connected to.

CHAPTER 3

ROBOT DESIGN

3.1 Requirements Definition

To guide our design process, we developed a set of requirements for our system.

- **SR1.** The system's outer diameter must not exceed four centimeters.
  Given that the average adult laryngeal inlet is 4-5 cm wide, our device must fit within this range to be suitable for laryngeal surgery as a surgical robot.

- **SR2.** The system shall support the use of existing flexible microsurgery devices.
  A variety of compliant microsurgery devices exist for use in commercial endoscopes and are readily available.

- **SR3.** The system shall provide the operator with the ability to simultaneously control three microsurgery devices within the surgical workspace.
  This capability allows for efficient multitasking during surgical procedures, enhancing the device's utility and versatility.

- **SR4.** The system shall not have any electromechanical components en vivo.
  Placing electromechanical components inside the patient introduces risk of harm during surgical procedures.

- **SR5.** The system should provide the operator a clear visualization of the pathway and surgical workspace, independent of the tools used and their placement.
  During surgery, the surgeon needs to be able to see the workspace they are operating in.

- **SR6.** The full material costs of the full system shall cost no more than $1000.
  A lower-cost system is more replicable and iterable, and more likely to be adopted by hospitals.
- **SR7.** The system's components shall not undergo plastic deformation during actuation.
  Plastic deformation leads to permanent changes in material shape, which is unacceptable for a surgical device

3.2 Design Overview

Our design, depicted in Figure 3.1, comprises two subsystems: the End Effectors with their actuation unit and the Flexible Laryngoscope Robot. The Flexible Laryngoscope Robot functions similarly to a traditional laryngoscope by opening up the surgical workspace and creating a clear path for surgical tools. However, it offers added flexibility, by way of a manipulable flexible wrist Figure 3.2, during the insertion of the device into the larynx. The end effectors are concentric agonist-antagonist robots (CAARs), shown in Figure 3.5, a type of soft robot made of two concentric tubes with opposing cuts into the tubing that allow for bending when the inner of the two tubes is displaced with respect to the outer tube [31]. Our design utilizes Polytetrafluoroethylene (PTFE) tubing for these CAARs, which was picked due to its low coefficient of friction and high availability in varying sizes.

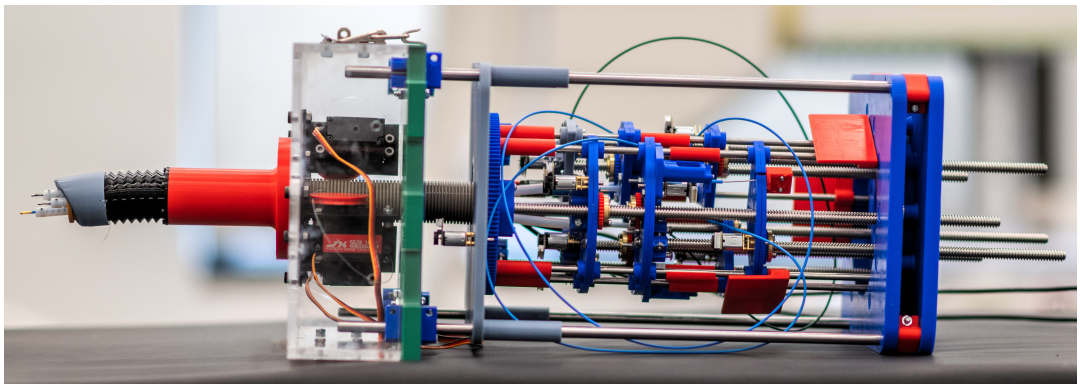

Figure 3.1: *Fully-assembled FASTR robotic device.*

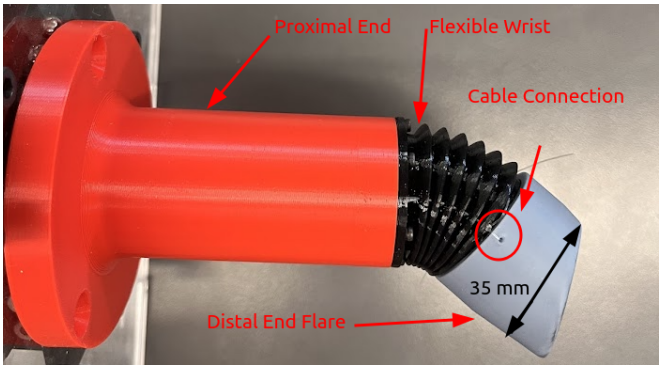

Figure 3.2: *Flexible wrist bending.*

3.3 Flexible Laryngoscope Robot

To deliver the end effectors and cameras to the surgical workspace, a device that mimics the functions of a typical laryngoscope is required. As shown in Figure 1.1, the laryngoscope is inserted through the oral opening and provides a clear, linear path for surgical instruments.

The shape and form factor of existing micro-laryngeal instruments along with the required visuals to perform surgery drive the typical micro-laryngoscope to be a straight hollow piece of metal. In the case of FASTR, both of these requirements are met using flexible components: visuals are provided by two cameras in a stereo configuration (see Section 3.7), and the typical surgical instruments are traded for similarly sized cable-driven tools housed in flexible manipulators, shown in Figure 3.5. Thus allowing for the design and implementation of a flexible laryngoscope robot to perform similar actions to a typical laryngoscope but in a more compliant geometry.

3.3.1 Design Theory

The flexible laryngoscope consists of three main parts: the distal end flare, the flexible wrist, and the proximal end. Given the anatomy of the throat and larynx, its most beneficial to have increased curvature towards the distal end of the laryngoscope. This is because the anatomy narrows as it approaches the vocal cords and trachea. Therefore, the proximal end is a long rigid piece that supports the flexible wrist. This design ensures that bending the wrist affects only the direction of the distal end.

The concept of the distal end flare in the flexible laryngoscope was inspired by typical micro-laryngoscopes. After the flexible joint, the distal end flare is a rigid piece tapered to one side. This design creates a soft point that is particularly beneficial during laryngoscope insertion. It effectively pushes tissue away from the surgical area and supports any tissue that might naturally droop into the workspace. Figure 1.2 illustrates a typical micro-laryngoscope, which also features a similar soft point at its distal end to assist with tissue clearance and device insertion into the surgical area.

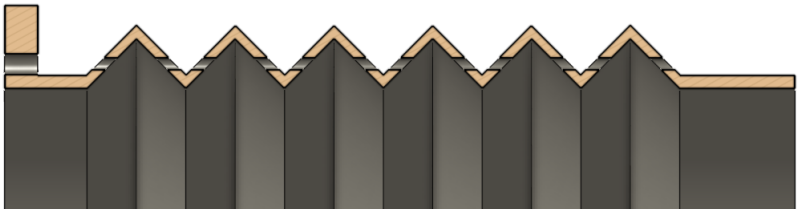

Figure 3.3: *Cross-section of the flexible wrist joint.*

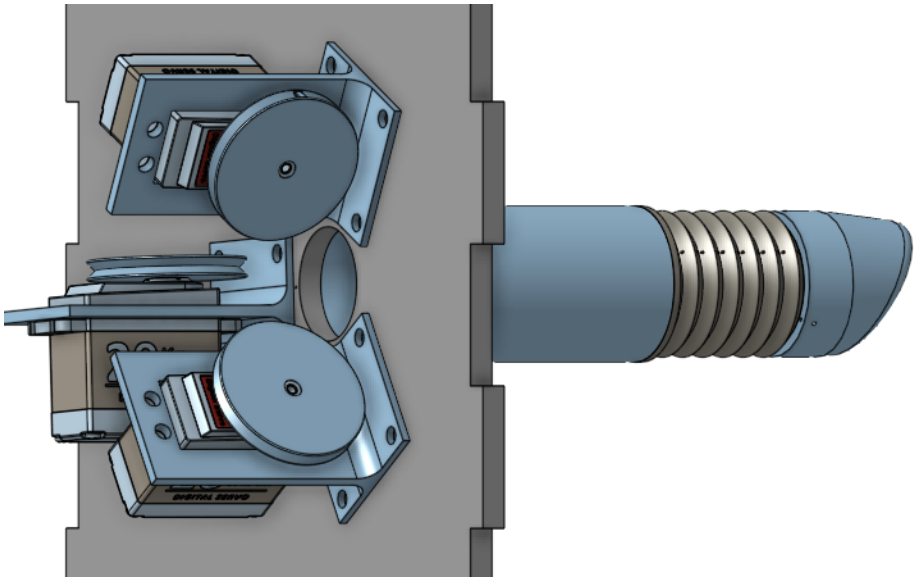

Figure 3.4: *CAD model of servo placement with respect to flexible servo laryngoscope.*

Lastly, the flexible wrist, shown in Figure 3.2, is a circular piece of 3D-printed Thermoplastic polyurethane (TPU, a flexible and durable material) with an accordion-like cross-section, shown in Figure 3.3. This shape allows for the flexible wrist to be actuated with the use of three cables, spaced 120° apart along the perimeter of the flexible joint, which when pulled or released creates flexion in the direction of the cable.

3.3.2 Flexible Wrist Actuation

Three rotary position servos are used with drums to pull on the cables running through the flexible wrist, figure 3.4 shows a layout of the positions of the servos. To achieve a specific deflection magnitude and direction of the wrist, the position command for each servo must be calculated using the geometric approach outlined in Section 3.6.

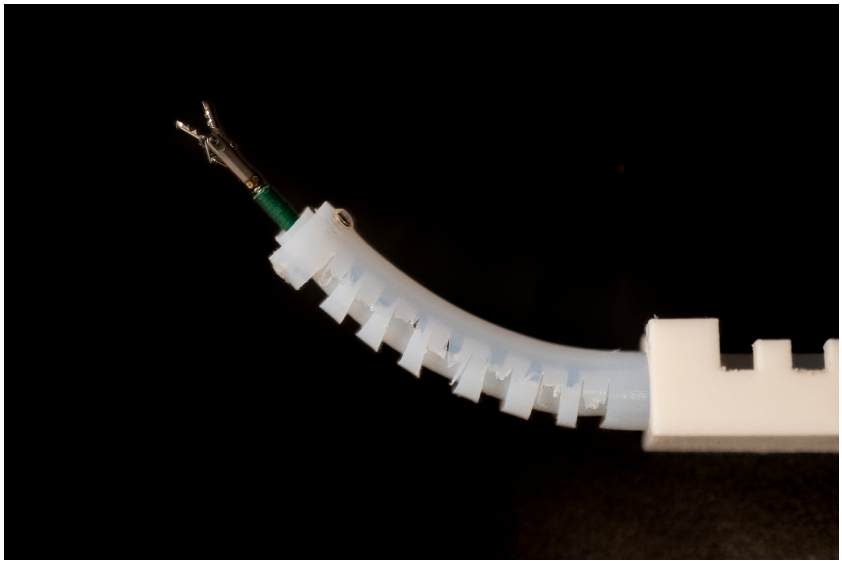

Figure 3.5: *Concentric agonist-antagonist robot.*

3.4 End Effectors

3.4.1 Design Theory of Concentric Agonist-Antagonist Robots (CAARs)

Concentric agonist-antagonist robots, shown in Figure 3.5, provide manipulability of the surgical tool head at the distal end of the robot, within the surgical workspace. Since translation and rotation are required for the whole tool head, and the bending is only required at the distal end, the team designed and manufactured CAARs from PTFE tubing, cutting the notch patterns at one end and routing the cables through a flexible housing to the actuation unit.

During a surgical procedure, being able to move a tool head throughout its entire actuation range is imperative. Consequently, a critical requirement derived is that there should be no plastic deformation occurring within that actuation range. This ensures that the device maintains its structural integrity and functionality throughout the procedure, thereby ensuring patient safety and the effectiveness of the surgical tool.

To calculate the maximum notch depth that resists plastic deformation at a given bending angle we use a geometric approach. First, we calculate the centroid of the notched portion of the CAAR, shown in Figure 3.6, using the following equation:

$$\bar{y} = \frac{4}{3}\left(r_o \frac{\sin^3 \frac{\theta_2}{2}}{\theta_2 - \sin\theta_2} - r_i \frac{\sin^3 \frac{\theta_1}{2}}{\theta_1 - \sin\theta_1}\right) \tag{3.1}$$

This centroid, determined by Equation 3.1, serves as the neutral axis for our stress calculations.

Next, to find the strain at the most strained portions of the CAAR notch—specifically, the outer and inner edges of both the outer and inner tubes—we adopted the approach from Oliver-Butler et al. [31]. With the strain on the outer and inner edges calculated, we use the following equation to find the equivalent stress due to strain:

$$\gamma_{eq} = E \cdot \epsilon \tag{3.2}$$

where ϵ, γ_{eq}, $and\, E$ are strain, equivalent stress, and young's modulus respectively.

The analysis above was used to calculate the specific notch profile of our outer and inner tubes which had outer and inner dimensions as listed in Table 3.1. For our analyses, we used a Young's modulus (E) of 575 MPa and a yield strength of 96 MPa. We set the plastic deformation strain limit at 0.4 based on findings from [32], who reported a compression strain limit of approximately 0.4 for extruded PTFE. Additionally, [33] indicated a tension strain limit for PTFE of around 0.5.

For our particular notch profile, we calculated that at a bending angle of 90°, the maximum strain reached 0.086, resulting in a strain safety factor of 4.65. By applying Equation 3.2, we calculated a maximum stress of 49.45 MPa, resulting in a stress safety factor of 1.94.

Tube Outer Diameter (mm)	**Tube Inner Diameter (mm)**	**Tube Maximum Notch Depth, h_2 (mm)**
7	5	3.1
4	2	2.4

Table 3.1: *Maximum Notch Depths for Inner and Outer Tube Configurations.*

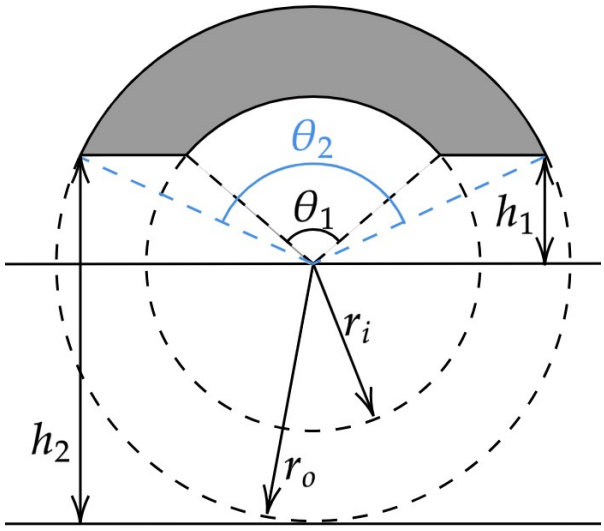

Figure 3.6: *Concentric agonist-antagonist robot notch cross-section.*

3.4.2 Manufacturing CAARs

Our early CAAR tubes were fabricated on an SLA 3D printer, but due to the limited surface area and the lack of adhesive receptivity of PTFE tubing (the material used to transfer motion from the actuation unit to the CAARs) an alternative solution was found for the manufacturing of CAARs.

Instead of fusing a separately manufactured CAAR to a PTFE tube, the CAAR notch profile for the inner and outer tube is cut out of the PTFE tubing itself at the distal end. This prevented issues associated with securing different materials to PTFE. To cut out the properly sized notches, a negative of the desired notch profile, shown in Figure 3.7, was designed to allow for a scalpel to penetrate the PTFE tubing until the desired point of notch height. At the distal end, the tubes are secured to each other with a pin through both the inner and the outer tubes (shown in Figure 3.8), while the proximal end of the tubes are held and displaced by the actuation unit.

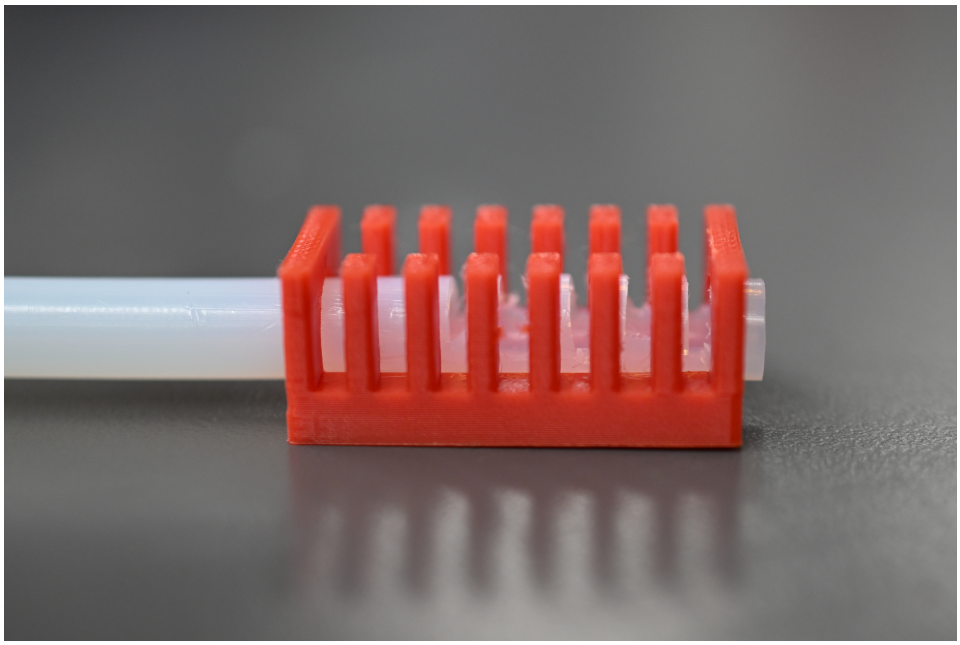

Figure 3.7: *PTFE Tubing resting in the notch profile cutting guide.*

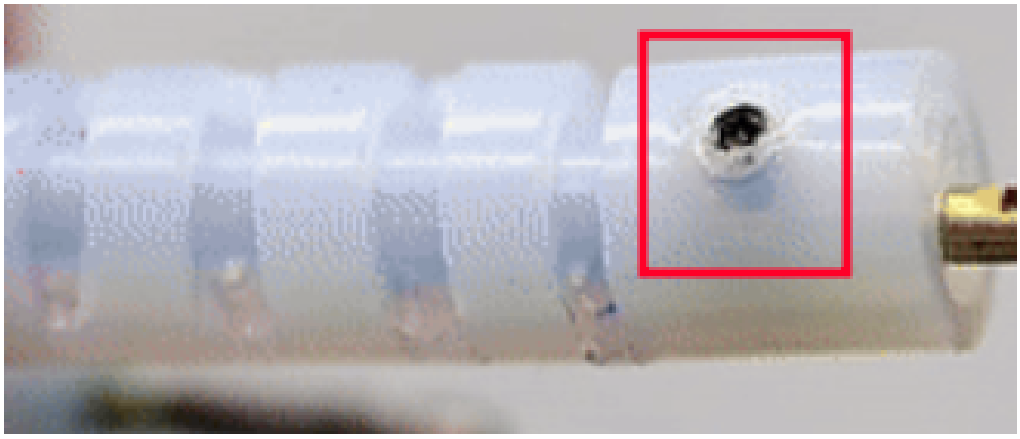

Figure 3.8: *Closeup of CAAR with headless socket holding the inner and outer tubes together.*

3.5 End Effector Actuation Unit

To actuate the CAARs one actuation mode is required: pulling or pushing the inner tube in relation to the outer tube. To maneuver or rotate the entire surgical tool head, the outer tube needs translation or rotation. Cable-driven instruments, on the other hand, operate by manipulating a cable within the surgical tool. Thus, precise adjustment of the cable's position relative to the tool's end is crucial for actuation. The actuation unit must therefore manage the absolute position of the outer tube, the relative motion between the inner and outer tubes, and the position of the surgical tool head's driving cable relative to the inner tube.

The actuation unit drives three identical manipulators, necessitating three identical systems to power each end effector. Lead screws were chosen for their ability to facilitate relative linear displacement. They provide a straightforward and reliable means of converting rotary motion from an electric motor into linear motion.

To both hold and manipulate a given cable or tube, the team designed a set of three plates, shown in Figure 3.9 the first plate for the outer tube, the second for the inner tube, and the third for the driving cable of the surgical tool head.

A 3D-printed adapter, shown in Figure 3.10, is used to securely hold the inner and outer tubes of the CAARs and fixture them to moving components to produce actuation. This adapter allows small headless set screws to secure the PTFE tubing (shown as fixture holes in Figure 3.10) both linearly and rotationally once the PTFE tubing is passed through the central lumen of the adapter. Given the PTFE tubing's inherent slipperiness, this secure connection is vital for stable positioning and movement within the CAARs system. Small clips on the design prevent the adapter from slipping out of the bearing. These clips ensure the bearing snaps securely onto the adapter, creating a stable connection with the PTFE tube. The design accommodates various bearing sizes and tubing diameters.

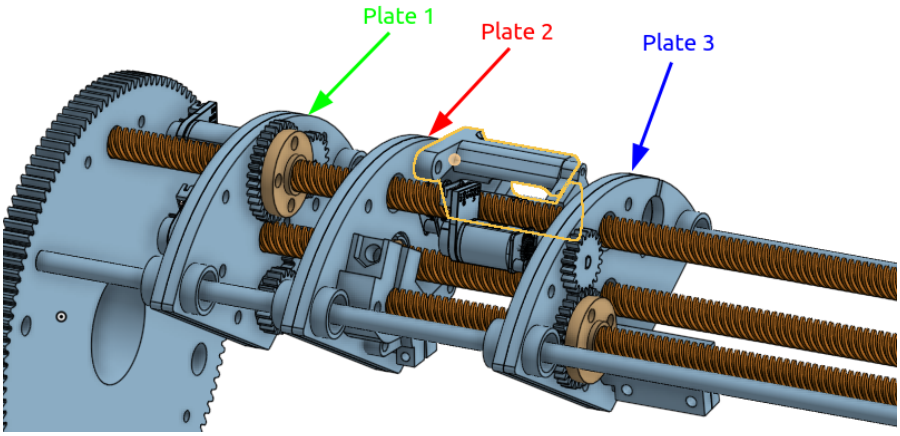

Figure 3.9: *CAD diagram of actuation plates for a single end effector.*

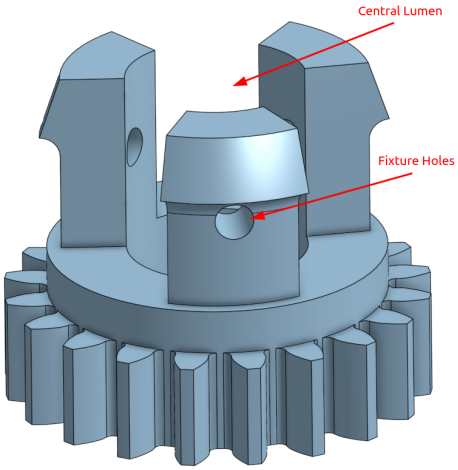

Figure 3.10: *CAD diagram of PTFE tubing adapter.*

The first plate, depicted in Figure 3.10, holds the outer tube using the previously mentioned adapter. This plate houses mounts for two motors: one adjusts the plate's linear position by turning a gear connected to a threaded nut on a lead screw, while the other rotates the outer tube using a specialized adapter with an integrated gear pattern. Additionally, this plate holds another lead screw with a 3D-printed clamp. The lead screw fixed to stage one is used by stage two for linear translation, rather than sharing the same lead screw as stage one. Motors on this plate control the end effector's rotation and translation.

Separately attached lead screws simplify relative actuation by driving each subsequent stage from a lead screw securely fixed to the prior stage, shown in Figure 3.11. This design avoids the complexity of coordinating movements on a single lead screw, which could lead to system failure if not managed correctly.

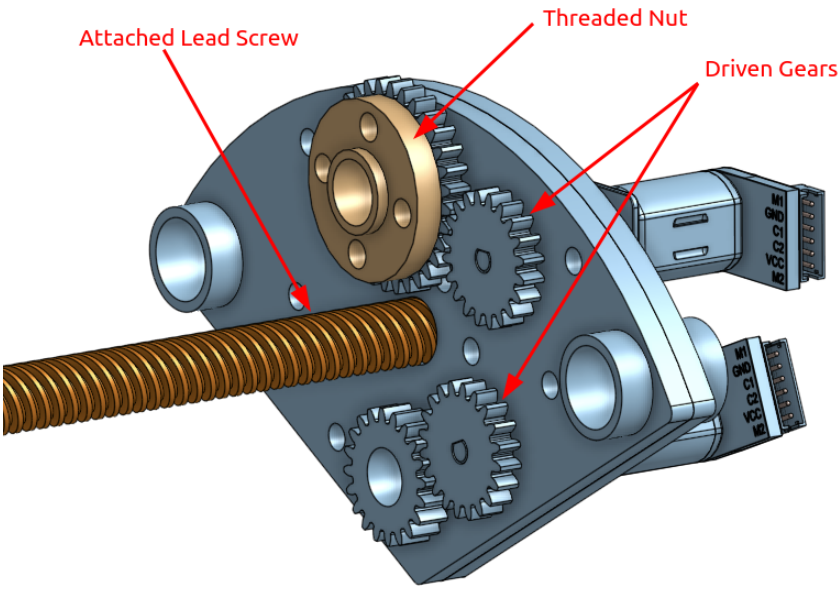

Figure 3.11: *CAD diagram of plate one and all driving components.*

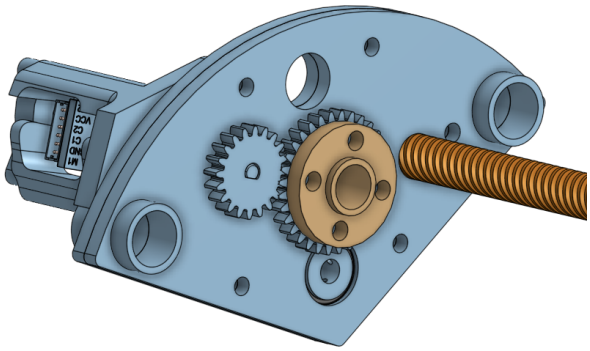

Figure 3.12: *CAD diagram of plate two and all driving components.*

The second plate, shown in Figure 3.12, linearly secures the inner tube while allowing free rotation via the PTFE tubing adapter. It features a single motor mount, with the motor rotating a threaded nut on the lead screw connected to the first plate. This plate also houses a lead screw for the third stage. The plate's movement controls the bending axis, depicted in Figure 3.5, of the surgical tool manipulator.

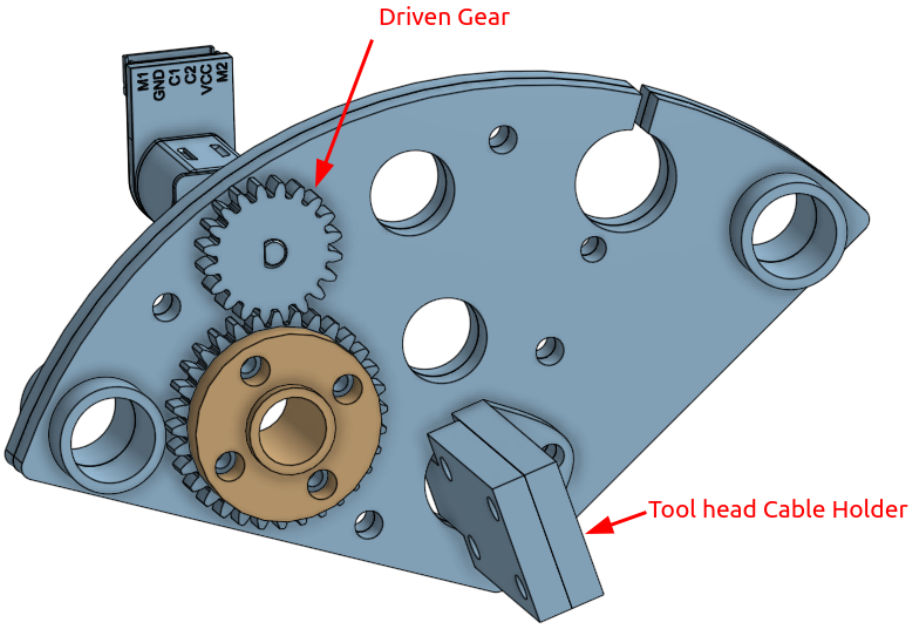

Figure 3.13: *CAD diagram of plate three and all driving components.*

The third plate, shown in Figure 3.13, houses the driving cable for the surgical tool head. Since the driving cable freely rotates within the surgical tool's housing, no bearing or adapter is needed. This plate includes a motor mount for a motor that rotates a threaded nut on the lead screw connected to the second plate. The plate's movement controls the opening and closing of a surgical tool.

The team used biopsy forceps, as shown in Figure 3.14, for the FASTR's surgical tools. This choice was primarily due to their availability, as these forceps are medical-grade and therefore expensive. However, the team designed the CAAR actuation unit such that any tool head can be adapted. Similar to CAAR actuation, there is an outer and inner part that, when moved relatively to each other, results in grasping actuation. Specifically for the surgical tools, there is a wire kept within a tightly wound spring where the inner wire connects to each forcep jaw. The outer spring is secured to the second stage of the CAAR actuation unit, while the forceps wire is attached to the third stage. When stage three is moved away from stage two, the wire pulls on the jaws to close. Conversely, when stage three moves towards stage two, the wire pushes the jaws outward.

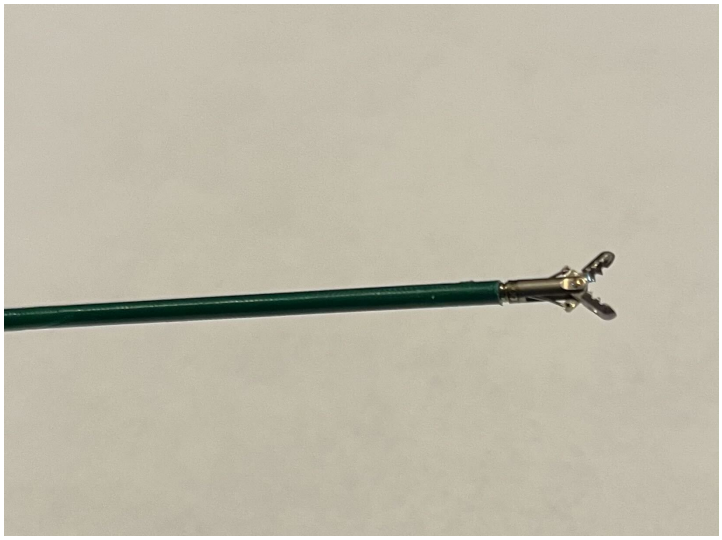

Figure 3.14: *Photo of biopsy forceps tool head.*

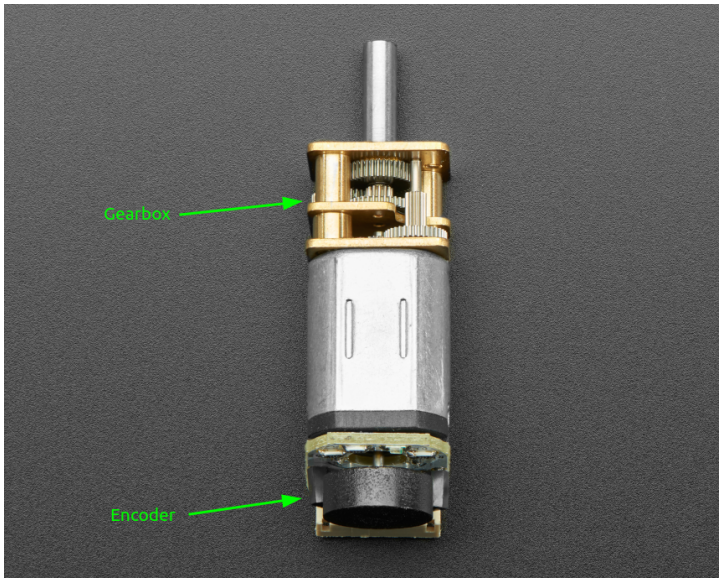

Figure 3.15: *Photo of a N20 dc motor with attached magnetic encoder*
"N20 DC Motor with Magnetic Encoder" by Adafruit Industries CC BY-NC-SA 2.0 DEED.

The motors employed in the design are N20 DC motors with magnetic encoders, shown in Figure 3.15. For the prototype, a specific configuration with a 300 rpm no-load speed was used as it offered the best performance in terms of power delivery. Quadrature encoders enable dual-direction position tracking. Integrated with the control software and an H-bridge circuit, the motor operates in servo mode. In this mode, the master Raspberry Pi sends position commands for a plate relative to its preceding plate, which the controller then maintains, which results in joint-space control for the end user.

3.6 Control Electronics and Structure

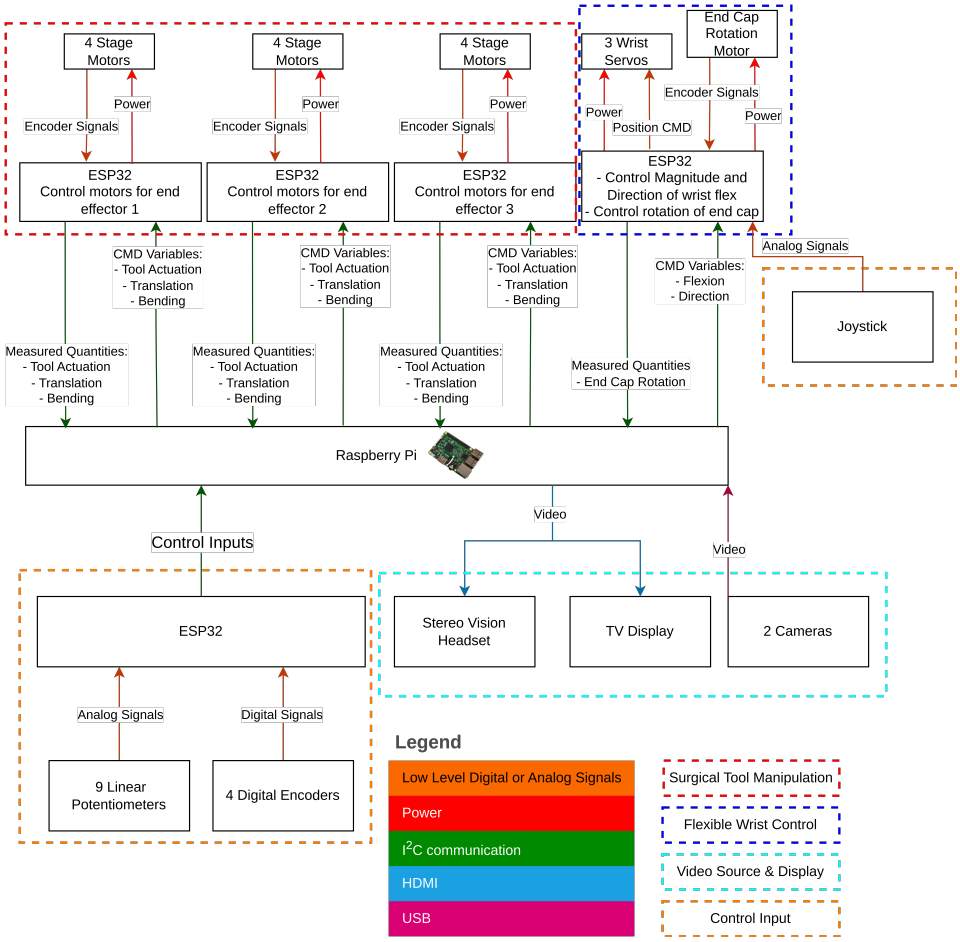

Figure 3.16: *High level diagram of electronics and communication Structure.*

There are two separate entities that can be physically manipulated to control the robot. The control board is the set of potentiometers and encoders used to control the individual CAARs and the overall sheath system containing the CAARs. The physical configuration of the control board is a three-grouping setup of three potentiometers and one encoder for each of the three CAARs with an additional rotary encoder at the top center of the board. An ESP32 is used to read the thirteen control inputs and send the readings as floats to the master Raspberry Pi. Each CAAR has four modes of actuation and thus each has four physical control inputs. Linear potentiometer sliders are used to control linear motion across the threaded rods in the CAAR actuation unit. The three types of motion controlled by linear potentiometers and thus by the relative motion of the three stages are CAAR translation, CAAR bending, and tool manipulation (the opening and closing of the surgical tool). Each of these actuation modes control a preset range of translation along the threaded rods. Rotary encoders are used to control the rotation of individual CAARs as well as the orientation of the complete CAARs system. This was intentionally made to be

intuitive because rotary encoders have infinite rotation, which translates to infinite rotation of the CAARs and CAARs system.

The second entity of the control system is a two-DOF joystick which is used to control the laryngoscope robot. There are two linear potentiometers attached to the joystick which map to x- and y-values. By converting the cartesian coordinates to polar coordinates, the polar coordinates can be mapped to two motors based on the angular distances between each motor the polar coordinate is between. When the angle is exactly in line with a motor, that motor is given 100% of the efforts interpreted from the joystick and the other two motors are held open.

The second control system actuates and controls the laryngoscope robot. The inputs to this system are a two-DOF joystick where x_j and y_j are in the range $[-100:100]$. First, equation 3.3 is used to compute the required deflection angle.

$$\phi = atan2(y_j, x_j) \tag{3.3}$$

Then equation 3.4 is used to compute the magnitude of bending and normalize to unity.

$$m = \frac{sat_0^{100}(\sqrt{x^2+y^2})}{100} \tag{3.4}$$

Once inputs are realized and processed, the end result is a deflection angle,$\phi[-\pi:\pi]$, that describes the commanded direction and a magnitude, $m[0:1]$, that describes the amount of bending in the commanded direction.

ϕ	R_1 Servo #	R_2 Servo #
$[\frac{\pi}{6} : \frac{5\pi}{6}]$	1	2
$[-\frac{\pi}{2} : \frac{\pi}{6}]$	2	1
$[-\frac{\pi}{2} : \frac{5\pi}{6}]$	3	2

Table 3.2: *Servo Routing Matrix.*

To determine the servo commands based on a given set of inputs, we employ a geometric approach. Each servo produces a deflection vector, denoted as R, which is proportional to the retraction of its cable. We solve the system of equations formed by equations 3.5 and 3.6 to calculate R_1 and R_2, corresponding to the retraction commands for servo 1 and servo 2, respectively, while any two servos are active (retracting), the third servo is set to zero. This is illustrated graphically in Figure 3.17. When the control vector falls directly in between two servos, the solutions for R are both equal to $\frac{\sqrt{3}}{2}$, which is the absolute maximum value for R. As such a scale of $\frac{2}{\sqrt{3}}$ is applied to R values to compute the percent actuation for each servo.

It's important to note that this method is valid only when ϕ falls within the range $[\frac{\pi}{6}, \frac{5\pi}{6}]$. To handle values of ϕ outside this range:

- For ϕ in the interval $[-\frac{\pi}{2}, \frac{\pi}{6}]$, we add $\frac{4\pi}{6}$ to ϕ and solve for R_1 and R_2 and then allocate the resulting servo commands to the appropriate servos based on Table 3.2.
- For ϕ in the interval $[-\frac{\pi}{2}, \frac{5\pi}{6}]$, we add $\frac{8\pi}{6}$ to ϕ and solve for R_1 and R_2 and then allocate the resulting servo commands to the appropriate servos based on Table 3.2.

$$U_x = R_1 cos(\frac{\pi}{6}) + R_2 cos(\frac{5\pi}{6}) \tag{3.5}$$

$$U_y = R_1 sin(\frac{\pi}{6}) + R_2 sin(\frac{5\pi}{6}) \tag{3.6}$$

On-board an ESP32, all these calculations are performed. The ESP32 uses an ADC to read data from the joystick and sends PWM signals to control the servo positions. For each servo, we determine a zero offset, $offset_\theta$, which represents the point where further movement would cause bending of the wrist or functionally zero percent actuation. Additionally, we experimentally establish the actuation range, r_a, which defines the safe limits for the servo's movement to prevent damage to the wrist while bending. Then, given an actuation percent R, solved for above, the ESP32 uses equation 3.7 to calculate the servo position command. This ESP32, shown in figure 3.16 in a blue dashed rectangle, is also responsible for handling the rotation of the entire CAAR actuation unit.

$$\theta_{command} = offset_\theta + r_a * R \tag{3.7}$$

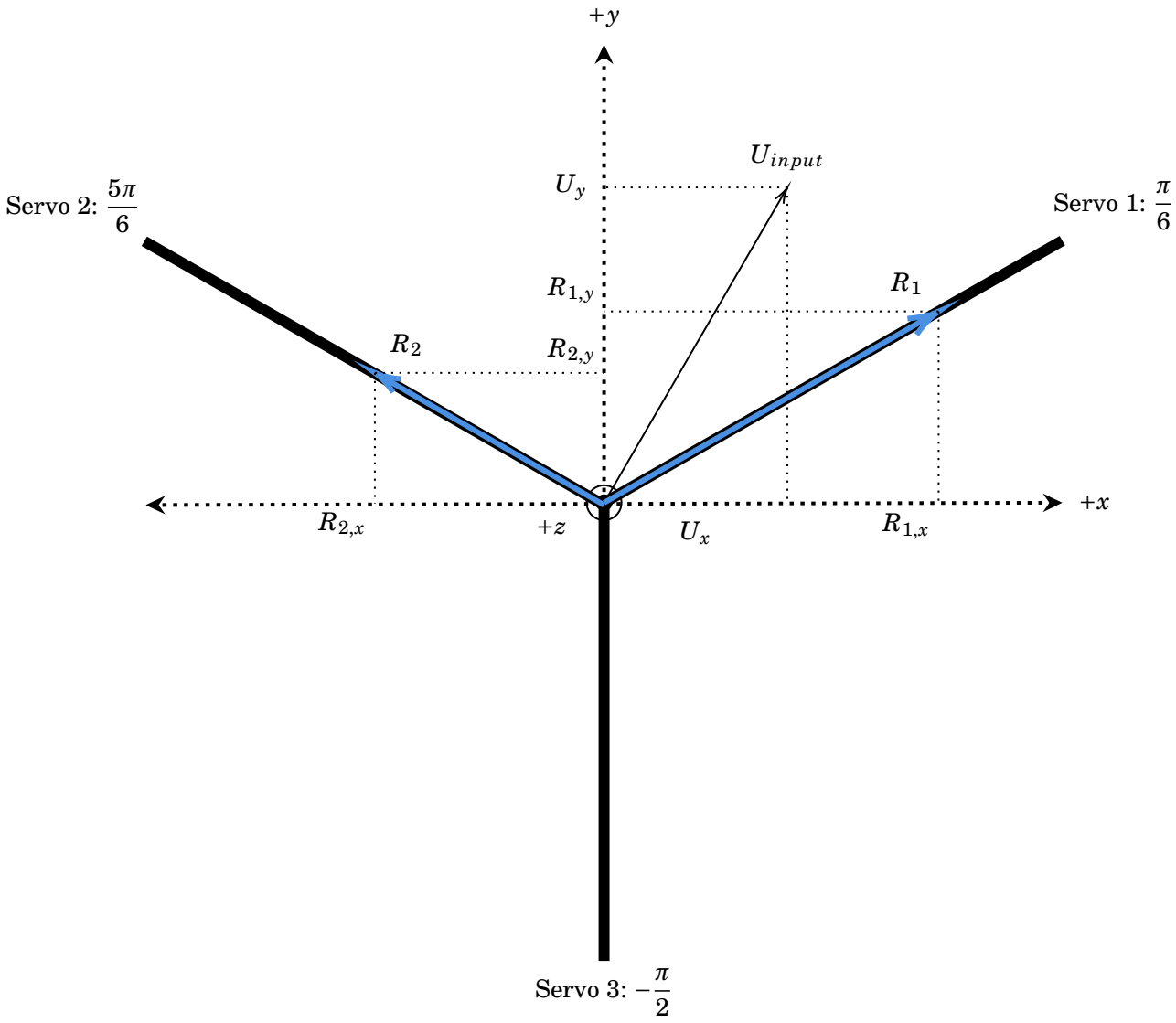

Figure 3.17: *Mapping joystick values to servo movements.*

Figure 3.18: *Photo of robot end cap.*

3.7 Stereo Vision

A stereo camera setup with two cameras mimics human binocular vision. This allows surgeons to perceive depth and spatial relationships accurately. In laryngeal surgery, where precision is paramount, this means a surgeon can more effectively judge the distance between structures within the larynx, minimizing the risk of unintentional damage and preserving the minimally-invasive nature of this surgery. This study showed that using stereo video to assist minimal-access robotic surgery using the Da Vinci surgical suite improved surgical accuracy and efficiency. To create the stereo vision setup, a pair of 640 × 480 pixel endoscopy cameras were secured to the end cap of the surgical device, with a baseline of 2 cm and tilted 5 degrees from normal, which was found to focus the stereo vision with minimal parallax at the working distance. This is shown in Figure 3.18.

The user interface for the vision setup is a proof-of-concept aimed to present the surgeon with stereo vision with few features, since in a later revision of this device the stereo camera setup would likely be its own subunit acquired separately. The user interface consists of a Sony HMZ-T3W [34], an external display, and a computer capable of running Python (≥ 3.6), as well as the Python program itself. The Sony HMZ-T3W is a head-mounted display capable of delivering stereo or mono video to the viewer through two 720p screens, one for each eye.

The program begins by assessing the displays connected to the computer, and presenting prompts on all screens, and the user presses any key until the HMZ-T3W's screen contains a window saying it is the head-mounted display, after which they press space. After, the program attempts to select which two cameras attached to the computer are the stereo cameras, since there could be a webcam or other unused camera drivers connected that the program can detect in addition to the desired cameras. It does this by taking an image from each camera, convolving a 41×41 Gaussian kernel over each to perform a heavy blur, comparing the photometric (per-pixel) error between each pair of images, and returning the pair with the lowest photometric loss. If the chosen set of cameras is not the desired pair, the user can specify the indices of the correct ones through the serial console of the Python program, but this is generally avoided by positioning an object in front of the end cap of the robot to make the camera's views as similar as possible. A structural similarity index comparison is an option that was explored, but is computationally expensive and not realistically required for this level of precision comparing camera views for correct registration [35].

At this point, the HMZ-T3W should be set up to interpret display input as side-by-side 3D video, and one of the camera's video feeds is displayed on the external monitors(s). A few keys on the keyboard are set up to perform modifications to the camera input to help the viewer: 'M' changes the view from stereo to monocular vision, and pressing 'Space' returns the view to stereo vision, 'S' swaps the cameras in case the eyes are flipped, and 'F" flips the camera views 180 degrees.

CHAPTER 4

INTEGRATION AND TESTING

4.1 CAARs Testing

With the FASTR robot mechanically and electrically assembled, testing then used the control box and laryngoscope joystick. Using the control box, each CAAR's 4 modes of actuation were tested. First, the desired range was adjusted in the ESP32 actuation and control software, and the physical stages were appropriately lined up. Then, the ESP32s were initiated and thus the potentiometer and encoder input values passed along I^2C were converted to motor efforts on each ESP32. The first and leftmost potentiometer of each grouping was slid from the zero position to the maximum to correspond with the translational movement of the CAAR from the tip of the laryngoscope robot's distal end to within the laryngoscope robot. Each tool was able to independently or simultaneously perform translation. The next actuation mode to test was CAAR bending, the principal characteristic of CAARs. The next test of actuation was done by rotating the entire CARR-tool pairs. Each tool was able to independently or simultaneously rotate with the rotation of the associated rotary encoder. Testing CAAR bending was completed by homing the second stages relative to the first stages and initializing the central potentiometers to the center of its range. Bending occurs by moving the potentiometer away from the center and towards one of the extremes, which correlate to stage displacement and thus CAAR bending. Each tool was able to independently or simultaneously perform bending. Finally, the grasping, or opening and closing, of each tool head was evaluated with the rightmost linear potentiometer. As expected, the tool heads were able to be manipulated by the translation of stage 3 relative to stage 2. Thus, every individual mode of actuation was able to be performed and thus the requirement of having three end effectors with four functional actuation modes each was met.

An essential analysis performed for the CAARs was plastic deformation analysis. A requirement of the CAARs was to have no plastic deformation through ± 90° bending. This was because the team wanted their design to meet or exceed the reachable workspace of current transoral systems. The factor of safety for both the strain and stress were 4.6 and 1.8 respectively, which means the CAAR bending is limited by stress. Despite a stress limit, the CAARs were tested via the control box to confirm no plastic deformation at 90° in either direction. Given 20 tests of bending between full deflection in one direction and then the other, no noticeable deformation was observed.

4.2 Laryngoscope Robot Testing

The laryngoscope robot was also tested to verify the code for controlling the three motors was performing as expected given specific joystick inputs. Due to limited time and resources, the team was only able to acquire joysticks with a significant dead band. When supplied with 3V or 5V, the potentiometers that make up the x- and y-efforts of the joystick jumped from about 20% to 100% effort in proximity to the joystick's center. While the joystick can be used, for testing the team opted to send deflection command programmatically. Figure 4.1 shows the results of a test where the distal end of the laryngoscope robot was commanded to a constant bending magnitude of 15° with a varying deflection direction. This graph demonstrates how the controller maintains a constant bending magnitude while varying the deflection.

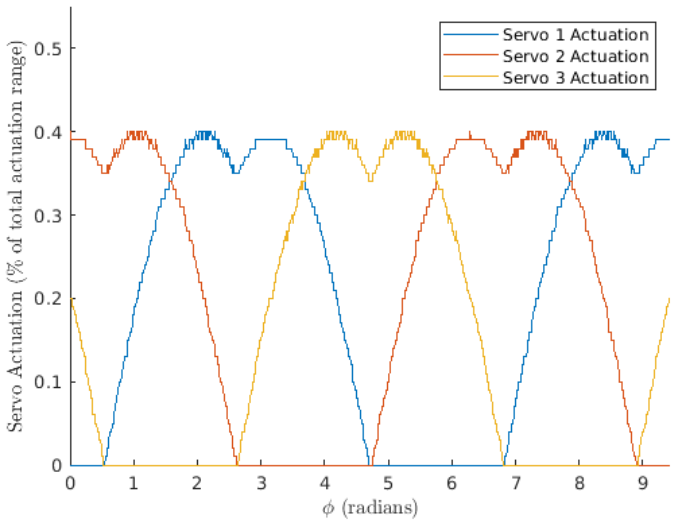

Figure 4.1: *Graph showing the three servo efforts versus deflection direction for the laryngoscope robot.*

Another test performed was an analytical test on the laryngoscope's bending abilities. Given that the flexible wrist has a relaxed length of 40 millimeters and the actuation range of the bellows is 26 millimeters, the maximum deflection angle was calculated to be 49°. This means that the laryngoscope robot is able to bend 49^{o} with respect to the insertion plane which is 49^{o} more than a typical, rigid laryngoscope. The flexible laryngoscope that the team developed has the potential to be more applicable for transoral surgeries currently being performed and surgeries that presently cannot be completed transorally due to patient anatomy.

CHAPTER 5

DISCUSSION AND FUTURE WORK

5.1 Requirements Analysis

Table 5.1 shows a comprehensive list of our requirements and how we met or did not meet them along with a short description of the work that was performed to meet a certain objective.

5.2 Discussion

In this project, the team aimed to develop a novel transoral robotic surgery device tailored for laryngeal surgery, particularly for the removal of cancerous laryngeal tumors. This paper presents our efforts to design and test a comprehensive system capable of providing the operator with control over three independent end effectors or surgical tools within the surgical workspace, while also offering a curved path to the larynx instead of a linear one.

Additionally, our device enhances surgical visualization by offering a stereoscopic, or 3D, view of the surgical workspace. This advanced visualization capability is complemented by a monocular view which is accessible to both surgeons and assistants. Together, these viewing options aim to improve surgical precision and facilitate better decision-making during procedures.

To enhance the minimally invasive nature of current surgical techniques, our device incorporates a flexible laryngoscope robot with nearly a 50° deflection angle. This feature allows the path of insertion to the larynx during a laryngeal procedure to be more adaptable to a patient's anatomy. The increased compliance of our device enables minimally invasive laryngeal surgery to be performed on a broader range of patients with varying laryngeal anatomies.

Requirement	Completed?	Summary of Work
SR1	✓	The team was able to maintain a maximum of 3.5 cm diameter through the entire portion of the device that enters the patient
SR2	✓	The team successfully demonstrated the opening and closing of biopsy forceps during manipulation (translation, rotation, and bending) of the surgical tool head.
SR3	✓	Each surgical tool head is controlled by its own microcontroller, receiving and acting on commands simultaneously. The team successfully demonstrated the simultaneous manipulation of all three surgical tool heads.
SR4	✓	There are no electromechanical components placed inside the patient during a proposed surgical operation with FASTR
SR5	✓	Two stereo cameras at the distal end of the system provide the operator with both binocular and monocular view of the surgical workspace
SR6	x	The development and testing of this project took approximately $250 of additional funding received from COMET Lab
SR7	✓	Through a full range of ±90° of bending, no plastic deformation is experienced using the notch profile the team designed for our system's end effectors

Table 5.1: *Requirements Results Table.*

For optimal surgical instrument dexterity during the procedure, we utilized concentric agonist-antagonist robots with surgical tools passed through the lumens of these robots. Our actuation unit grants the operator complete control over the translation, rotation, bending, and grasping of the surgical tool within the surgical workspace.

Our device is currently in the prototype stage as it requires further development in terms of manufacturing and custom parts before extensive testing. Nonetheless, we have demonstrated the legitimacy and feasibility of the actuation modes and concepts within a surgical setting.

5.3 Future Work

Our goal for this project was to create a prototype platform for performing TORS in the larynx. We successfully manufactured a robotic device that actuates three individual surgical tools while providing a surgeon with a 3-dimensional visualization of the surgical workspace and allows for emergency reversion to manual surgery. While we met many of our requirements, we have recommendations for future work that can be done to improve the abilities of the system.

5.3.1 Ex-Vivo Testing

Future work should primarily focus on conducting extensive testing of the laryngoscope robot in an ex-vivo environment. This testing would include cyclic fatigue testing, in which the laryngoscope robot would be actuated continuously while bending through its 360 degree range to develop estimations of product lifetime due to mechanical fatigue. This information would provide customers of the product important information about when they need to replace this component of the robotic system to ensure the system's reliability during surgery. Furthermore, cyclic fatigue testing should be performed on the CAARs to also determine when the CAARs should be replaced to ensure mechanical fatigue is not reached and components of the robotic system operate and respond as intended.

5.3.2 Custom-Manufactured Equipment

Future iterations of this project could include custom parts such as printed circuit boards (PCBs) and special surgical tools. Using custom-manufactured PCBs would bring the project a step closer to becoming a complete product, and the wiring complexity would be greatly reduced. Also, as the iterations progress, the existing 3D-printed parts should be manufactured out of metal as the robotic system progresses to become a commercial product.

5.3.3 User Interface

Another important focus of future work is to develop a more comprehensive user interface for a surgeon's operation of the robotic system. The current user interface was designed for simplicity as the main focus of this project was to conceptualize, design, manufacture and determine the viability of the FASTR robotic system. However, future iterations of the FASTR system should include a more intuitive user interface developed through consulting multiple ENT surgeons that often perform laryngeal surgeries. Intuitively mapping all degrees of freedom of the FASTR system to a user interface may prove difficult, but one potential solution is a three joystick system, where each joystick is responsible for all actuation of one CAAR. The rotation of the entire robotic system, and bending of the laryngoscope robot, could then be mapped to extra buttons on the joysticks or operated with separate controllers. Additionally, the VR headset used during operation could include a heads-up display that provides information to the surgeon

about the component of the robot they are currently operating, such as a 2D sketch view of the movement of a CAAR during actuation.

5.3.4 CAARs Manufacturing

Future iterations of the FASTR system should aim to reduce the size of the CAARs. Diametrically smaller CAARs would allow for better visualization of the surgical space during surgery using the stereo camera system. Also, smaller CAARs would allow for more maneuverability of the surgical tools within the larynx, and would allow for the diameter of the laryngoscope robot to decrease to allow the FASTR system to be less invasive and/or used on younger individuals with smaller anatomy. One method of reducing the diametric size of the CAARs is by manufacturing them out of nitinol tubing. Desired notch profiles can be laser cut out of the nitinol tubes to create the outer and inner tubes comprising CAARs. However, this manufacturing method is more expensive and time-consuming than manufacturing the CAARs out of PTFE tubing.

5.3.5 External Support

Finally, future FASTR iterations could mount the robotic system to manually operated supporting arms. The current FASTR system was designed to support this feature, but was not able to be tested using it due to time and budget constraints. Mounting the FASTR system to overhead arms in an operating room would allow for easier manual manipulation of the system by the surgeon to insert the robot into the patient for surgery. Mounting arms would also aid in the emergency situation where the CAARs are removed to allow for manual surgical operation. With mounting arms, the CAARs and CAAR actuation unit could be easily detached from the laryngoscope robot and quickly moved out of the way to allow for manual operation.

5.4 Ethics

5.4.1 Environmental

When individuals undergo manual or robotic transoral laryngeal surgery, they are often subject to in-hospital recovery times lasting multiple days. These recovery times are necessary to monitor the patients to ensure the surgery was successful and no complications arise, but each patient in a hospital bed affects the hospital's environmental footprint. For example, a patient in the ICU (intensive care unit) generates 7.1 kg of solid waste and 138 kg CO2 per bed per day [source]. These emissions mostly are due to energy consumption, hospital equipment purchase and usage, food, and hospital staff travel. Therefore, the FASTR system aims to decrease a hospital's environmental footprint by providing a method for laryngeal surgery that reduces the average postoperative hospital stay for patients by eliminating the need for supine positioning of the patient. Also, patients of laryngeal surgery are benefited directly by quicker recovery times and resulting lower hospital costs. However, as most of the FASTR system is 3D printed from PLA, the manufacturing of the product may impact the health of local populations. Through the process of biological magnification, if the product is disposed of improperly and the plastic is broken or degraded into microplastics and enters the food chain, the plastic from the product may be consumed in harmful quantities by humans as the concentration of the plastic increases in higher trophic levels of the food chain.

5.4.2 Social

Although the FASTR system is made to be used on and aid patients with laryngeal tumors, the system will positively impact other individuals as well. Doctors performing the surgery will be benefited as the system allows doctors to treat more patients with laryngeal tumors through a minimally invasive transoral method. Those that were predisposed to transoral surgery due to constrictive anatomy may now be able to get transoral laryngeal surgery, providing them with faster postoperative recovery times than the open-neck surgical method they would need without the FASTR system. Also, the FASTR system benefits the family of those undergoing laryngeal surgery, as they will not need to take care of their family member as long post operation. Family members will also likely be less stressed due to the surgery being minimally invasive as opposed to the invasive open-neck method that may cause various surgical complications. One downside of the FASTR system is its cost when compared to manual surgical methods, but the system is cheaper to manufacture and use than the Da Vinci system and saves patients and hospitals costs through shorter in-hospital recovery times. Finally, the FASTR system aims to combat healthcare disparities by providing a system that can offer minimally invasive laryngeal surgery to a wider range of patients.

5.4.3 Global

The FASTR system is a product that would be useful worldwide given that 1 in 40 people, throughout the world, are affected by laryngeal tumors [source from fact from pres]. With some of these individuals being predisposed to current transoral laryngeal surgical methods, a system that provides a form of minimally invasive surgery to more individuals worldwide would greatly aid the population. Therefore, this product will be demanded in the global market to aid a wide range of laryngeal surgery patients.

5.4.4 Economic

One issue with transoral robotic surgery is the cost, as the Da Vinci system is expensive to manufacture and use. However, the FASTR system is significantly cheaper to manufacture with the proof of concept version exhibiting a total cost of around 700 dollars for all parts. Furthermore, using the Da Vinci system would save hospitals money as the hospital does not need to pay to purchase and upkeep the Da Vinci system or pay for long postoperative in-hospital stays for laryngeal surgery patients. In terms of healthcare disparities, the FASTR system allows for more individuals to be treated than other minimally invasive surgical transoral methods. The system is more cost effective and the surgery using the device can therefore be afforded by more people with laryngeal tumors.

BIBLIOGRAPHY

[1] B. Chakravarthy and W. Seipp, *Direct Laryngoscopy*. Cham: Springer International Publishing, 2022, pp. 55–60. [Online]. Available: https://doi.org/10.1007/978-3-030-85047-0_9

[2] Teleflex Corporation, "Ent instruments catalog." [Online]. Available: https://teleflex.widen.net/s/lc6zjvplkl/mc-002206-pilling-ent-instruments-catalog

[3] H. E. Eckel and M. Remacle, "Fundamentals of laryngeal surgery: Approaches, instrumentation, and basic microlaryngoscopic techniques," *Textbook of Surgery of Larynx and Trachea*, p. 37–45, 2022. [Online]. Available: https://link.springer.com/chapter/10.1007/978-3-031-09621-1_4

[4] US Government, "Conducting passages of the human respiratory system." [Online]. Available: https://en.wikipedia.org/wiki/Respiratory_tract#/media/File:Illu_conducting_passages.svg

[5] Defense Visual Information Distribution Service, "The da vinci surgery system awaits its first surgery." [Online]. Available: https://picryl.com/media/the-da-vinci-surgery-system-awaits-its-first-surgery-782dc2

[6] J. H. Hah, S. Sim, S.-Y. An, M.-W. Sung, and H. G. Choi, "Evaluation of the prevalence of and factors associated with laryngeal diseases among the general population," *The Laryngoscope*, vol. 125, no. 11, pp. 2536–2542, 2015. [Online]. Available: https://onlinelibrary.wiley.com/doi/abs/10.1002/lary.25424

[7] Atrium Health, "Microscopic laryngeal microsurgery." [Online]. Available: https://www.wakehealth.edu/treatment/l/laryngeal-microsurgery

[8] Weill Cornell Medicine, "Microscopic laryngeal surgery." [Online]. Available: https://voice.weill.cornell.edu/treatments/surgery/microscopic-laryngeal-surgery

[9] M. M. Statham, A. L. Sukits, M. S. Redfern, L. J. Smith, J. C. Sok, and C. A. Rosen, "Ergonomic analysis of microlaryngoscopy," *The Laryngoscope*, vol. 120, no. 2, p. 297–305, Nov 2009. [Online]. Available: https://www.ncbi.nlm.nih.gov/pmc/articles/PMC4893949/

[10] A. T. Hillel, A. Kapoor, N. Simaan, R. H. Taylor, and P. Flint, "Applications of robotics for laryngeal surgery," *Otolaryngologic Clinics of North America*, vol. 41, no. 4, p. 781–791, Aug 2008. [Online]. Available: https://www.ncbi.nlm.nih.gov/pmc/articles/PMC4096143/

[11] M. Runciman, A. Darzi, and G. P. Mylonas, "Soft robotics in minimally invasive surgery," *Soft Robotics*, vol. 6, no. 4, p. 423–443, Aug 2019. [Online]. Available: https://www.ncbi.nlm.nih.gov/pmc/articles/PMC6690729/

[12] A. De Virgilio, A. Costantino, G. Mercante, F. Ferreli, P. Yiu, T. Mondello, D. Sebastiani, L. Malvezzi, R. Pellini, and G. Spriano, "High-definition 3-d exoscope for micro-laryngeal surgery: A preliminary clinical experience in 41 patients," *Annals of Otology, Rhinology amp; Laryngology*, vol. 131, no. 11, p. 1261–1266, Dec 2021. [Online]. Available: https://journals.sagepub.com/doi/10.1177/00034894211063741

[13] A. Majewicz and A. M. Okamura, "Cartesian and joint space teleoperation for nonholonomic steerable needles," in *2013 World Haptics Conference (WHC)*, 2013, pp. 395–400. [Online]. Available: https://ieeexplore.ieee.org/document/6548441

[14] Cleveland Clinic. What's in the (voice) box? [Online]. Available: https://my.clevelandclinic.org/health/body/21872-larynx

[15] J. Suárez-Quintanilla, A. Fernández Cabrera, and S. Sharma, "Anatomy, head and neck: Larynx," in *StatPearls*. StatPearls Publishing, Jan. 2024, [Updated 2023 Sep 4]. Available from: https://www.ncbi.nlm.nih.gov/books/NBK538202/.

[16] THANC Foundation. Supraglottic cancer anatomy thanc guide. THANC Guide Knowledge. Hope. Support. [Online]. Available: https://thancguide.org/cancer-types/throat/laryngeal/supraglottic/anatomy/

[17] Cleveland Clinic. What is the epiglottis? function & anatomy. [Online]. Available: https://my.clevelandclinic.org/health/body/24278-epiglottis

[18] C. Hacking. Subglottis: Radiology reference article. Radiopaedia. [Online]. Available: https://radiopaedia.org/articles/subglottis?lang=us

[19] MD Anderson Cancer Center. Throat cancer. The University of Texas MD Anderson Cancer Center. [Online]. Available: https://www.mdanderson.org/cancer-types/throat-cancer.html

[20] M. Rubinstein and W. B. Armstrong, "Transoral laser microsurgery for laryngeal cancer: A primer and review of laser dosimetry," *Lasers Med Sci*, vol. 26, pp. 113–124, 2011. [Online]. Available: https://doi.org/10.1007/s10103-010-0834-5

[21] R. K. Orosco, K. Tam, M. Nakayama, F. C. Holsinger, and G. Spriano, "Transoral supraglottic laryngectomy using a next-generation single-port robotic surgical system," *Head & Neck*, vol. 41, no. 7, pp. 2143–2147, 2019. [Online]. Available: https://onlinelibrary.wiley.com/doi/abs/10.1002/hed.25676

[22] Intuitive. Intuitive for head and neck surgeons. Intuitive.com. [Online]. Available: https://www.intuitive.com/en-us/healthcare-professionals/surgeons/head-and-neck

[23] G. S. Weinstein, B. W. O'malley Jr, and N. G. Hockstein. (2005) Transoral robotic surgery: Supraglottic laryngectomy in a canine model. [Online]. Available: https://pubmed.ncbi.nlm.nih.gov/15995528/

[24] M. Ansarin, S. Zorzi, M. A. Massaro, M. Tagliabue, M. Proh, G. Giugliano, L. Calabrese, and F. Chiesa, "Transoral robotic surgery vs transoral laser microsurgery for resection of supraglottic cancer: a pilot surgery," *The International Journal of Medical Robotics and Computer Assisted Surgery*, vol. 10, no. 1, pp. 107–112, 2014. [Online]. Available: https://onlinelibrary.wiley.com/doi/abs/10.1002/rcs.1546

[25] E. E. Alon, J. L. Kasperbauer, K. D. Olsen, and E. J. Moore, "Feasibility of transoral robotic-assisted supraglottic laryngectomy," *Head & Neck*, vol. 34, no. 2, pp. 225–229, 2012. [Online]. Available: https://onlinelibrary.wiley.com/doi/abs/10.1002/hed.21719

[26] L. R. Schild, F. Böhm, M. Boos, L. A. Kahrs, J. Coburger, J. Greve, L. Dürselen, T. K. Hoffmann, and P. J. Schuler, "Adding flexible instrumentation to a curved videolaryngoscope: A novel tool for laryngeal surgery," *The Laryngoscope*, vol. 131, no. 2, pp. E561–E568, 2021. [Online]. Available: https://onlinelibrary.wiley.com/doi/abs/10.1002/lary.28868

[27] N. G. Hockstein, J. P. Nolan, B. W. O'Malley Jr, and Y. J. Woo, "Robotic microlaryngeal surgery: A technical feasibility study using the davinci surgical robot and an airway mannequin," *The Laryngoscope*, vol. 115, no. 5, pp. 780–785, 2005. [Online]. Available: https://onlinelibrary.wiley.com/doi/abs/10.1097/01.MLG.0000159202.04941.67

[28] A. De Virgilio, Y. M. Park, W. S. Kim, S. J. Baek, and S.-H. Kim, "How to optimize laryngeal and hypopharyngeal exposure in transoral robotic surgery," *Auris Nasus Larynx*, vol. 40, no. 3, pp. 312–319, Jun. 2013. [Online]. Available: https://doi.org/10.1016/j.anl.2012.07.017

[29] P. T. Dziegielewski, S. Y. Kang, and E. Ozer, "Transoral robotic surgery (tors) for laryngeal and hypopharyngeal cancers," *Journal of Surgical Oncology*, vol. 112, no. 7, pp. 702–706, 2015. [Online]. Available: https://onlinelibrary.wiley.com/doi/abs/10.1002/jso.24002

[30] C. A. Solares and M. Strome, "Transoral robot-assisted co2 laser supraglottic laryngectomy: Experimental and clinical data," *The Laryngoscope*, vol. 117, no. 5, pp. 817–820, 2007. [Online]. Available: https://onlinelibrary.wiley.com/doi/abs/10.1097/MLG.0b013e31803330b7

[31] K. Oliver-Butler, J. A. Childs, A. Daniel, and D. C. Rucker, "Concentric push–pull robots: Planar modeling and design," *IEEE Transactions on Robotics*, vol. 38, no. 2, pp. 1186–1200, 2022. [Online]. Available: https://par.nsf.gov/servlets/purl/10347432

[32] J. L. Jordan, C. R. Siviour, J. R. Foley, and E. N. Brown, “Compressive properties of extruded polytetrafluoroethylene,” *Polymer*, vol. 48, no. 14, pp. 4184–4195, 2007. [Online]. Available: https://www.sciencedirect.com/science/article/pii/S0032386107004752

[33] C. Luo, J. Pei, W. Zhuo, Y. Niu, and G. Li, “Phase transition behavior and deformation mechanism of polytetrafluoroethylene under stretching,” *RSC Adv.*, vol. 11, pp. 39 813–39 820, 2021. [Online]. Available: http://dx.doi.org/10.1039/D1RA06333B

[34] Sony Corporation, “Sony hmz-t3w head mounted display reference guide.” [Online]. Available: https://www.sony.com/electronics/support/res/manuals/4471/44719771M.pdf

[35] Z. Wang, A. C. Bovik, H. R. Sheikh, and E. P. Simoncelli, “Image quality assessment: From error visibility to structural similarity,” Apr 2004. [Online]. Available: https://www.cns.nyu.edu/pub/lcv/wang03-reprint.pdf

APPENDIX A: AUTHORSHIP

Section	Title	Author
1	Introduction	Samay Govani
1.1	Current Surgical Procedure	Chase Beausoleil
1.2	Existing Robotic Surgery Devices for Laryngeal Procedures	Chase Beausoleil
1.3	Paper Outline	Everyone
2.1	Client Statement	Mark Gagliardi
2.2	Relevant Anatomy	Chase Beausoleil
2.3	Existing Methods for Laryngeal Procedures	Mark Gagliardi
2.4	Existing Instruments for Laryngeal Procedures	Mark Gagliardi
3.1	Requirement Definition	Cole Parks
3.2	Design Overview	Samay Govani
3.3	Flexible Laryngoscope Robot	Samay Govani
3.4	End Effectors	Samay Govani
3.5	End Effector Actuation Unit	Samay Govani
3.6	Control Electronics and Structure	Samay Govani
3.7	Stereo Vision	Cole Parks
4.1	CAARs Testing	Mark Gagliardi
4.2	Laryngoscope Robot Testing	Mark Gagliardi
5.1	Requirements Analysis	Samay Govani
5.2	Discussion	Samay Govani
5.3	Future Work	Chase Beausoleil
5.4	Ethics	Chase Beausoleil